J. Plasma Physics (2006), *vol.* 72, *part* 6, *pp.* 1041–1044. © 2006 Cambridge University Press
doi:10.1017/S0022377806005186 Printed in the United Kingdom

Adaptive finite elements for a set of second-order ODEs

JAKUB URBAN and JOSEF PREINHAELTER
EURATOM/IPP.CR Association, Institute of Plasma Physics, Prague, Czech Republic

(Received 15 August 2005 and accepted 27 December 2005)

Abstract. A Hermite finite-elements approach with adaptive mesh refinement for the solution of a set of second-order ordinary differential equations is described. The main advantage of the method is its usability for stiff equations with boundary conditions. For cases where exponentially growing solutions can exist, the method overcomes the common problems of initial value solvers. The method was successfully used for the full-wave solution of wave propagation in inhomogeneous plasma where the mode conversion process between ordinary, extraordinary and electron Bernstein waves occurs.

1. Hermite finite elements for second-order ordinary differential equations

In addition to the more commonly used ordinary differential equation (ODE) solvers (e.g. Runge–Kutta), the finite-elements method (FEM) can also be used to solve ODEs. Although it is generally more complicated, it brings several advantages and can overcome some of the problems of other methods. In particular, since it is a natural boundary value problem, we do not need any special technique for adapting an initial values solver. This is a valuable advantage for problems where more solutions may exist, e.g. exponentially growing and decaying waves. The method is also suitable for stiff equations.

For ODEs with solutions continuous up to the first derivative, the cubic Hermite polynomials provide adequate discretization [1]. To solve a set of m second-order ODEs with an n-node mesh $x_1 \dots x_n$, the unknown functions f_k are discretized as

$$f_k(x) = \sum_{i=1}^{n} \left(K_k^i G_0(\xi_i) + L_k^i G_1(\xi_i) \right), \quad k = 1 \dots m, \tag{1.1}$$

where $G_0(\xi_i) = (|\xi_i| - 1)^2(2|\xi_i| + 1)$, $G_1(\xi_i) = (|\xi_i| - 1)^2 \xi_i h_i$ are the Hermite finite elements (Fig. 1), K_k^i, L_k^i are the unknown coefficients, $\xi_i = (x - x_i)h_i^{-1}$ and

$$h_i = \begin{cases} x_i - x_{i-1}, & x \in \langle x_{i-1}, x_i \rangle, \\ x_{i+1} - x_i, & x \in \langle x_i, x_{i+1} \rangle. \end{cases} \tag{1.2}$$

Using the Galerkin approach, the ODEs are transformed to linear algebraic equations for the K_k^i, L_k^i coefficients. The matrix of the problem is a $2mn \times 2mn$ $(6m - 1)$-diagonal matrix. Such a system can be solved efficiently by LU decomposition. Implementations can be found in various numerical libraries, e.g. DLSLCB from the IMSL Fortran Library (used in our code) or ZGBSV from

https://doi.org/10.1017/S0022377806005186 Published online by Cambridge University Press

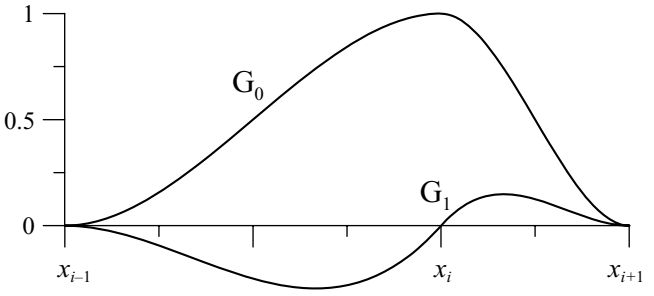


Figure 1. Cubic Hermite finite elements.

LAPACK. In fact, the matrix contains only $8m^2n$ non-zero elements, but a special solver for such a matrix would be needed to take advantage of that.

In the computation, much more computer time is used for the matrix elements evaluation, whereas the solution of the band matrix is very fast. Each matrix element is computed separately, with no interaction with the other elements. Thus, the algorithm can be easily parallelized by using different processors for different parts of the computational mesh.

2. Adaptive mesh refinement

An algorithm for the adaptive mesh refinement based on the local error estimation has been developed [2]. The error estimates are computed as the maximum norm of the difference of two solutions computed on different meshes. In detail, we construct a local deviation vector for the (l) mesh

$$\mathbf{d}_i^{(l)} = \max_{k=1\ldots m} \frac{\left|f_k^{(l)}\left(x_i^{(l)}\right) - f_k^{(l-1)}\left(x_i^{(l)}\right)\right|}{\max\limits_{i=1\ldots n^{(l)}} \left|f_k^{(l)}\left(x_i^{(l)}\right)\right|}, \tag{2.1}$$

where $i = 1\ldots n^{(l)}$, $x_i^{(l)}$ are the (l) mesh nodes and $f_k^{(l)}$ are solutions on the (l) mesh. If the global error

$$\Delta^{(l)} = \max_{i=1\ldots n^{(l)}} \left(\mathbf{d}_i^{(l)}\right) = \left\|\mathbf{d}_i^{(l)}\right\| \tag{2.2}$$

is greater than the desired accuracy δ, $\mathbf{d}$ is transformed in the following way:

$$\mathbf{d}'^{(l)}_i = \frac{\max\left(\mathbf{d}_i^{(l)} - \delta, 0\right)}{\Delta^{(l)}}(\eta_1 - \eta_0) + \eta_0, \tag{2.3}$$

where $\eta_0 > 1$, $\eta_1 \geqslant \eta_0$. Then the new $(l+1)$ mesh is constructed with node distances

$$x_j^{(l+1)} - x_{j-1}^{(l+1)} = \frac{x_i^{(l)} - x_{i-1}^{(l)}}{\mathbf{d}'^{(l)}_i}, \quad x_{i-1}^{(l)} \leqslant x_{j-1}^{(l+1)} \leqslant x_i^{(l)}. \tag{2.4}$$

Thus, η_0 and η_1 determine the node distance reduction in the lowest and in the highest error regions, respectively. These numbers must be adjusted according to the specific problem, but the method is not very sensitive to their small variations and values that are usable for a wide range of similar problems can be found.

https://doi.org/10.1017/S0022377806005186 Published online by Cambridge University Press

3. Wave propagation in cold magnetized plasma

3.1. Electron Bernstein Wave X–O mode conversion

For propagation of a harmonic 'plane wave'

$$\mathbf{E}(x,y,z,t) = \mathbf{E}(x,N_y,N_z)\exp[i(N_y y + N_z z - \omega t)]$$

in a cold magnetized plasma slab, inhomogeneous in the x direction, the following two ODEs for E_y, E_z must be solved:

$$\begin{aligned} &iN_y E_x' + \epsilon_{xy}E_x - E_y'' + \left(N_z^2 - \epsilon_{yy}\right)E_y - \left(N_y N_z + \epsilon_{yz}\right)E_z = 0,\\ &iN_z E_x' + \epsilon_{xz}E_x - E_z'' + \left(N_y^2 - \epsilon_{zz}\right)E_z - \left(N_y N_z + \epsilon_{yz}\right)E_y = 0,\\ &E_x = \left(-iN_y E_y' - iN_z E_z' + \epsilon_{xy}E_y + \epsilon_{xz}E_z\right)\left(N_y^2 + N_z^2 - \epsilon_{xx}\right)^{-1}, \end{aligned} \tag{3.1}$$

where $\epsilon_{\alpha\beta}$ is the cold plasma dielectric tensor. These equations can be used to estimate the X and O modes to electron Bernstein wave (EBW) conversion efficiency [3]. By introducing weak collisions, the singularity at the upper hybrid resonance (UHR) can be avoided and the energy collisionally absorbed at the UHR region is equal to the energy of the EBW. Nevertheless, the solution is almost singular at the UHR and a very fine mesh must be used there in the numerical solution. The O–X-EBW and EBW-X–O linear mode conversions are reciprocal processes; thus, in this way we can estimate the EBW-X–O conversion efficiency as well and use the results in EBW emission simulations [4,5]. Beyond the singularity at the UHR, (3.1) have an exponentially growing solution behind the UHR, which must be eliminated in our case [2]. For these reasons, it is troublesome to use standard ODE solvers, whereas the FEM described before fits well for this problem.

3.2. Properties of the adaptive method

To speed up the convergence, the initial mesh is proposed not as uniform, but with a Gaussian peak added in the UHR vicinity, so the initial mesh density is

$$n_0\left(1 + \alpha\frac{f}{\nu}\exp[-\beta^2(x - x_{\mathrm{UHR}})^2]\right), \tag{3.2}$$

where x is the depth in the plasma slab, x_{UHR} is the position of the UHR, f is the wave frequency, ν is the collision frequency, n_0 is an 'uniform mesh density', and α, β are the Gaussian shaping parameters. With such an initial mesh, the convergence can be considerably faster, as shown in Fig. 2.

The mesh property, which mostly determines the accuracy, is the peak at the UHR. For different initial meshes, the peak height is about the same for a given accuracy (Fig. 3), whereas the mesh density significantly differs in the rest of the domain.

4. Summary

A robust and effective FEM with adaptive mesh refinement algorithm for second-order ODE sets has been developed. The method is especially suitable for problems with strongly non-uniform mesh density requirements. Its usability and good performance have been shown for wave propagation in an inhomogeneous cold plasma slab, where studying EBW-X–O mode conversion requires solving almost singular ODEs.

https://doi.org/10.1017/S0022377806005186 Published online by Cambridge University Press

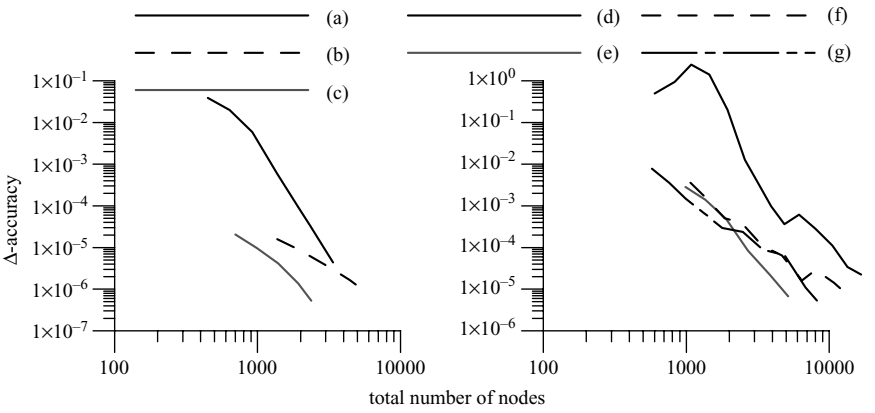


Figure 2. Convergence for NSTX shot 113544, 0.325 s. Left: $f = 10.5$ GHz, $\nu = 0.0005f$; (a) $n_0 = 300$, uniform initial mesh; (b) $n_0 = 300$, $\alpha = 0.015$; (c) $n_0 = 400$, $\alpha = 0.035$. Right: $f = 16.5$ GHz; (d) $\nu = 0.0005f$, $n_0 = 400$, uniform initial mesh; (e) $\nu = 0.0005f$, $n_0 = 400$, $\alpha = 0.035$; (f) $\nu = 0.0001f$, $n_0 = 300$, $\alpha = 0.015$; (g) $\nu = 0.0005f$, $n_0 = 300$, $\alpha = 0.015$. In all of the computations, $\beta = 7.5$, $\eta_0 = 1.2$, $\eta_1 = 1.8$.

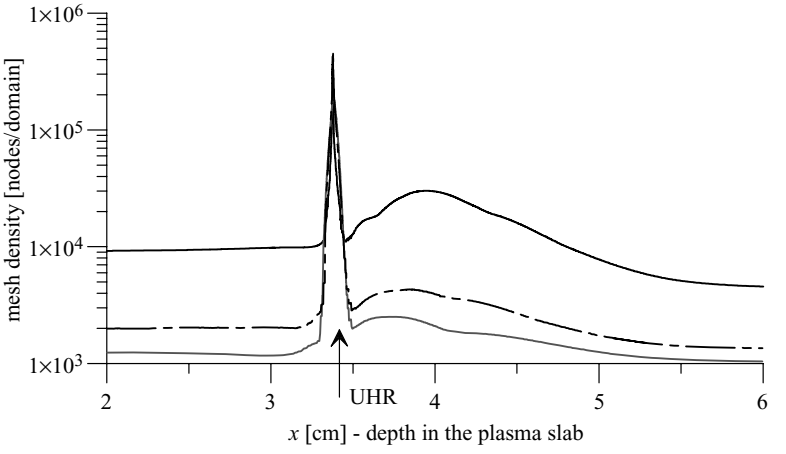


Figure 3. Mesh density for the cases (d), (e) and (g) from Fig. 2 for $\Delta \cong 10^{-4}$.

Acknowledgement

This work was supported by the Academy of Sciences of the Czech Republic, project AV0Z-20430508.

References

[1] Appert, K., Hellsten, T., Vaclavik, J. and Villard, L. 1986 *Comput. Phys. Communi.* **40**, 73–93.

[2] Urban, J. and Preinhaelter, J. 2004 *Czech. J. Phys.* **54**, C109–C115.

[3] Irzak, M. and Shcherbinin, O. N. 1995 *Nucl. Fusion* **35**, 1341–1356.

[4] Preinhaelter et al. 2004 *Rev. Sci. Instrum.* **75**, 3804–3806.

[5] Taylor, G. et al. 2005 *Phys. Plasma* **12**, 052511.

https://doi.org/10.1017/S0022377806005186 Published online by Cambridge University Press